NASA GRC High Power Electromagnetic Thruster Program

Michael R. LaPointe[1] and Eric J. Pencil[2]

[1]Ohio Aerospace Institute, 22800 Cedar Point Road, Cleveland, OH 44142
[2]NASA Glenn Research Center, 21000 Brookpark Road, MS: 301-3, Cleveland, OH 44135
Phone: (216) 433-6192, Fax: (216) 433-8311, Michael.LaPointe@grc.nasa.gov

Abstract. Interest in high power electromagnetic propulsion has been revived to support a variety of future space missions, such as platform maneuvering in low earth orbit, cost-effective cargo transport to lunar and Mars bases, asteroid and outer planet sample return, deep space robotic exploration, and piloted missions to Mars and the outer planets. Magnetoplasmadynamic (MPD) thrusters have demonstrated, at the laboratory level, the capacity to process megawatts of electrical power while providing higher thrust densities than current electric propulsion systems. The ability to generate higher thrust densities permits a reduction in the number of thrusters required to perform a given mission and alleviates the system complexity associated with multiple thruster arrays. The specific impulse of an MPD thruster can be optimized to meet given mission requirements, from a few thousand seconds with heavier gas propellants up to 10,000 seconds with hydrogen propellant. In support of NASA space science and human exploration strategic initiatives, Glenn Research Center is developing and testing pulsed, MW-class MPD thrusters as a prelude to long-duration high power thruster tests. The research effort includes numerical modeling of self-field and applied-field MPD thrusters and experimental testing of quasi-steady MW-class MPD thrusters in a high power pulsed thruster facility. This paper provides an overview of the GRC high power electromagnetic thruster program and the pulsed thruster test facility.

INTRODUCTION

Future in-space propulsion requirements for the orbit raising of large spacecraft, the economical delivery of lunar and Mars cargo, flexible outer planet rendezvous and sample return missions, and challenging new ventures in deep space robotic and piloted planetary exploration have renewed the national interest in the development and deployment of high power plasma propulsion systems. High power electromagnetic thrusters offer several potential advantages over chemical engines for each of these mission types (Gilland 1991, 1992; Filliben 1996; Oleson 1999), and the NASA Glenn Research Center (GRC) is working to develop high power (MW-class) electromagnetic thruster technologies to meet these demanding propulsion requirements. Current high power thruster research is focused on the magnetoplasmadynamic (MPD) thruster, and includes systems analysis, numerical thruster modeling, and experimental thruster testing. The primary numerical simulation tool used by GRC to predict and better understand MPD thruster performance is the MACH2 code (Mikellides, 1994).

Through a subcontract with the Arizona State University, MACH2 has been used to investigate MW-class self-field MPD thruster performance and is currently being used to understand the effects of applied magnetic fields on high power thruster operation. In a related effort, Kettering University is developing a numerical model of MPD thruster electrode sheath physics to enable predictions of the anode and cathode fall voltages. The electrode sheath voltages can be a significant fraction of the total thruster voltage at high power, and an accurate estimate of their magnitude is required to predict total thruster efficiency. Systems level modeling is performed through a cooperative agreement with the Ohio Aerospace Institute (Gilland, 2003), which is developing an analytic model of high power MPD thruster performance for use by systems designers and mission planners. At GRC, a high power thruster test capability has been established to provide rapid, economical testing of new MW-class MPD thruster geometries. The facility can provide up to 30-MW of pulsed power during a 2-ms discharge period, sufficient to establish quasi-steady thruster operation and allow accurate estimates of steady-state performance. This paper focuses on the design and operation of the high power test facility, and discusses preliminary results obtained with a baseline MW-class MPD thruster.

Magnetoplasmadynamic Thruster

In its basic form, the magnetoplasmadynamic (MPD) thruster consists of a concentric anode surrounding a central cathode (Fig. 1). A high-current arc is struck between the anode and cathode, which ionizes and accelerates a gas propellant. In self-field thrusters, the azimuthal magnetic field produced by the current returning through the central cathode interacts with the radial discharge current flowing through the plasma to produce an axial Lorentz body force, giving rise to the alternate sobriquet of Lorentz Force Accelerator (LFA) often encountered in the literature. In applied-field versions of the thruster, a solenoid magnet surrounding the anode provides additional radial and axial magnetic fields that can help stabilize and accelerate the plasma discharge.

Initially developed in the 1960's, the MPD thruster has been sporadically funded over the past few decades, leading to slow but steady improvements in performance. For a detailed history of MPD thruster development, the reader is referred to a number of review papers that chronicle the progress and challenge of this promising high power propulsion technology (Nerheim, 1968; Sovey, 1988; Myers, 1991). Various thruster geometries have been operated using a variety of propellants, with the most efficient performance to date achieved using lithium vapor propellant. Lithium-fed MPD thrusters developed by the Moscow Aviation Institute in Russia have reported efficiencies of around 45%, with specific impulse (Isp) values approaching 5000 s at power levels exceeding 100-kW (Tikhonov, 1997; Polk, 2000; Kodys, 2001; 2003; Sankaran, 2003). Facilities to investigate lithium-fed MPD thrusters have been established in the United States at the Jet Propulsion Laboratory and Princeton University, with experimental results soon to be forthcoming. While attractive from an efficiency viewpoint, a possible issue with lithium is that it is a condensable propellant with the potential to coat instrument surfaces and power arrays. In addition, the maximum achievable specific impulse (Isp) with lithium is around 7500 s, while future power-rich robotic and piloted outer planet missions will require specific impulse values approaching 10000 s.

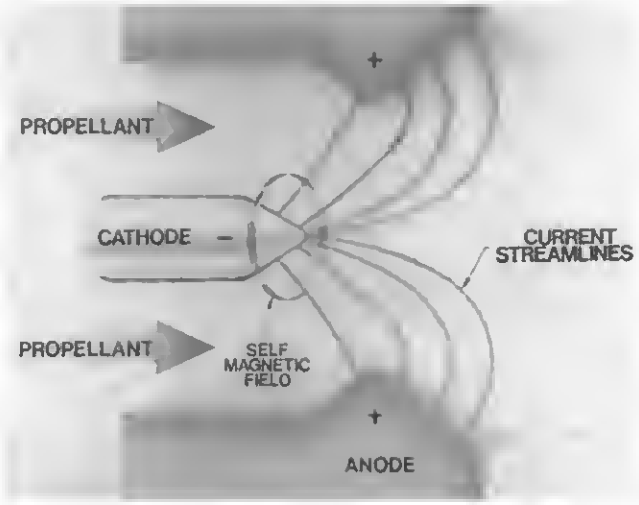

FIGURE 1. Self-field MPD Thruster Diagram.

These higher Isp values may be achieved with hydrogen, hence non-condensable gas propellants are also under investigation at various research facilities around the world to better understand and improve gas-fed thruster performance (Toki, 2002; Kinefuchi, 2003; Auweter-Kurtz, 1994; Winter, 2003; Zuin, 2003; Paganucci, 2003). Although gas-fed MPD thruster efficiencies have typically been lower than devices operated with lithium (Sovey, 1988; Myers, 1991; Choueiri, 1998), recent numerical models indicate that significantly improved performance can be achieved through the use of modified electrode geometries and the proper application of expansion nozzles and/or applied magnetic fields (Mikelliedes 2000a; 2000b; LaPointe, 2002). The use of non-condensable gas propellants mitigates possible ground handling and spacecraft contamination issues associated with lithium propellant, and may provide efficient thruster performance over a wide range of operating conditions. The NASA GRC effort is focused on the development and refinement of these high power gas-fed thruster technologies.

MPD THRUSTER TEST FACILITY

The high power plasma thruster test facility at the Glenn Research Center consists of a high-energy capacitor hank, pulse-forming network, vacuum chamher, thrust stand, and automated control systems. A brief description of each of the major facility elements is provided helow.

Pulse Forming Network

The pulse-forming network used for quasi-steady MPD thruster testing consists of 46 capacitors and 7 inductors arranged in a 7-element Guillemin network. Each capacitor is rated for 10-kVDC, with an expected shot life of 10^4 discharges at maximum charge voltage. The total hank capacitance is 4.88-mF, providing a maximum stored energy of 250-kJ at full charge. Switching is performed by a stack of solid-state thyristors rated for 15-kV and 50-kA peak current. Six of the inductors consist of insulated 0.95 cm (3/8") OD copper tuhing wound around short sections of 27.3 cm (10.75") OD pvc pipe; the seventh inductor, which channels most of the discharge current, is constructed of insulated 2-AWG stranded cahle. A 0.12-Ω matching resistor, rated for 10-kV and 250-kJ, is located in series between the switch and load. The capacitor hank and PFN are isolated from ground during each discharge. A 1000-Ω resistor rated for 250-kJ is tied into the hank via a relay switch and can be used to discharge the capacitors in the event of a thruster malfunction or safety interlock violation. The physical dimensions of the capacitor hank are 4.5 m (15 ft) long by 2.1 m (7 ft) high hy 0.9 m (3 ft) wide. A portion of the capacitor bank and PFN are shown in Fig. 2. The total discharge period is approximately $2x10^{-3}$ s, with less than 10% currcnt ripple over the discharge plateau. Representative current and voltage traces obtained with a 0.013-Ω resistive load used to simulate an MPD thruster discharge are presented in Fig. 3.

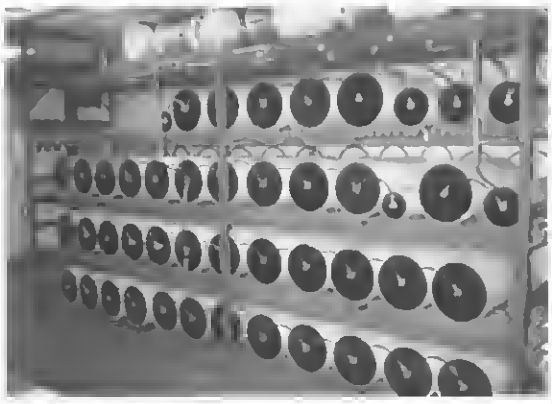

FIGURE 2. NASA GRC Capacitor Bank and PFN.

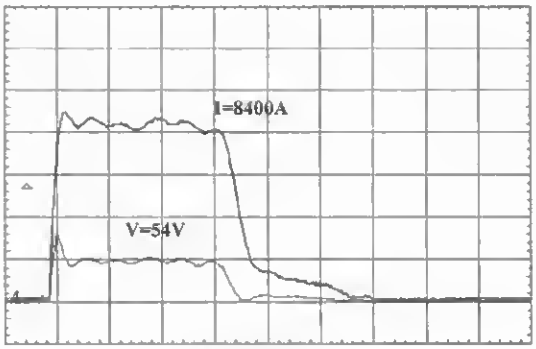

FIGURE 3. Capacitor Bank Discharge Voltage (V) and Current (I) into 0.013-Ω Resistor.

Vacuum Chamber and Propellant Plenum

Pulsed MPD thruster tests arc conducted in NASA GRC Vacuum Facility 1 (VF1). The vacuum chamher, shown in Fig. 4, is 1.5-m (5 ft) in diameter hy 4.5-m (15 ft) long. Access to the chamher interior is provided through an endcap mounted on a balanced swing-arm. The tank is pumped by two 0.8-m (32") diameter oil diffusion pumps and a mechanical roughing pump, and is capahle of reaching an unloaded base pressure of 10^{-6} torr ($8x10^{-9}$ Pa). The vacuum tank is locatcd on the floor ahove the capacitor hank, and powcr is cabled to the tank through high voltage feedthroughs located on a 1-m (36") bottom flange. Instrumentation and gas feedthroughs are located on a 0.4-m (16") side port, with additional access availahle through several 0.11-m (4.5") ports mounted to the facility endcap. A separate 0.4-m side port provides power cahle access for a magnetic field coil, descrihed in a later section of the paper.

The propellant gas plenum is mounted to a test cart located beside VF1 (shown in Fig. 4). The cylindrical plenum chamber is constructed of stainless steel, with an interior volume of 2.5×10^{-2} m^3 (1.5×10^3 in^3). Stainless steel tubing connects one end of the plenum to a regulated gas bottle, while the other end is connected to a pneumatic actuator powered by a fast acting solenoid valve. Gas flow from the actuator can be directed either to the thruster through a side flange located in VF-1, or to a small calibration chamber located on the test cart. Short sections of the propellant feed line are constricted to a nominal inner diameter of 1.6-mm (1/16") both upstream of the thruster and upstream of the calibration chamber, to ensure choked flow conditions are achieved along each propellant flow path. The stainless steel calibration chamber has an internal cylindrical volume of 6.1×10^{-3} m^3 (3.7×10^2 in^3) and is used to measure the amount of gas discharged during pulsed operation. Both the propellant plenum and the calibration chamber are outfitted with wide-ranging pressure gauges (dual pirani gauge and diaphragm manometer), capable of measuring pressure values from 10^{-3} torr to 1500 torr.

During calibration, the propellant plenum pressure is set to a given value, and the calibration chamber is evacuated to vacuum. Gas from the propellant plenum is discharged into the calibration plenum, and the resulting pressure rise is recorded. Knowing the pressure change and the chamber volume allows the propellant mass injected into the calibration chamber to be calculated, and dividing this mass by the total response period of the pneumatic actuator provides the propellant flow rate for the pulsed discharge. The flow period of the actuator can be set between 90-ms and 150-ms through the use of a variable resistor in the control circuit; a value of 110-ms is currently used to ensure the gas flow reaches the thruster and to reduce uncertainties in the actuator opening and closing response times. The plenum is presently rated for a pressure of approximately 1500-torr (2-atm), limiting the maximum argon mass flow rate to around 1.0-g/s.

As a second check on mass flow calibration, a fast-acting mass flow meter has recently been installed in the propellant feed line. The propellant plenum is set to a given pressure, and an electrical switch is used to open the actuator valve for a period of approximately 1-second, with propellant flow directed to the evacuated calibration chamber. Mass flow rates in units of sccm are measured and displayed by the mass flow meter, with values subsequently converted to mass flow rate in grams per second. As shown in Figure 5, the results of this independent calibration of mass flow rate are in excellent agreement with the linear curve fit to the volumetric flow rate calibrations, up to the measurement limit of the flow meter. Based on the combined flow meter data and the independently obtained calibration curve obtained with the calibration chamber technique, the mass flow rate is estimated to have an uncertainty of less than +/- 5%.

FIGURE 4. NASA GRC Vacuum Facility 1 (VF-1).

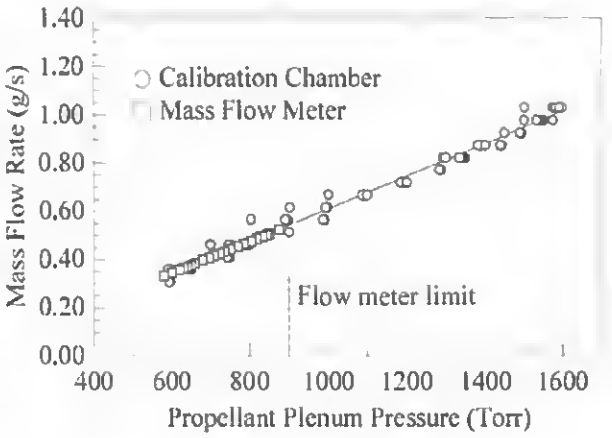

FIGURE 5. Argon Propellant Mass Flow Calibration.

Thrust Stand

The pulsed MPD thrust stand is based on a simple flexure design (Fig 6). The thruster is mounted to a stiff horizontal plate, which in turn is supported by four thin, contoured aluminum flexures mounted to a bottom support plate. Current is fed to the thruster through high voltage coaxial cables, with return currents traveling through the

cable shields to reduce magnetic tare forces on the thrust stand. During discharge, the upper plate of the thrust stand is horizontally displaced by the thruster impulse. To measure the resulting impulse, a calibrated dynamic load cell, mounted on a sturdy support hracket bolted to the hottom plate of the thrust stand, is placed in firm contact with the moveable upper plate of the thrust stand. Movement of the upper plate is restricted by contact with the load cell, and an oscilloscope measures the time-dependent voltage response of the load cell produced by the thruster impulse.

The thrust stand is calibrated prior to testing using a fixed-mount electronic impact hammer; the hammer tip impacts a separate dynamic load cell mounted on a cross bar spanning the face of the thruster anode, and the resulting impulse (time-integrated response) is measured hy the load cell on the thrust stand. The total impulse delivered by the impact hammer, as measured hy the impact load cell, is correlated to the total impulse of the thrust stand response, as measured by the thrust stand load cell. The resulting measurements provide a fourth-order polynomial calihration curve that can be used to determine thruster impulse (Fig. 7). Thrust stand measurements typically fall within +/-10% of the calibration curve.

The present thrust stand configuration does not allow in-situ calibration under vacuum conditions; however, a solid-state inclinometer mounted beneath the top plate of the thrust stand is used to provide information on the initial and final orientation (2-axis tilt) of the stand. No significant differences have been observed between thrust stand orientations at rest in air or under vacuum, providing some assurance that the measured impulse values will closely correspond to the calibrated thrust stand values. Nevertheless, to ensure accurate and repeatable placement of the thrust stand against the responding load cell, a vacuum-rated motion control actuator is currently being installed on the stand to provide consistent load cell compression against the thrust stand prior to obtaining impact hammer calibration or thruster impulse data.

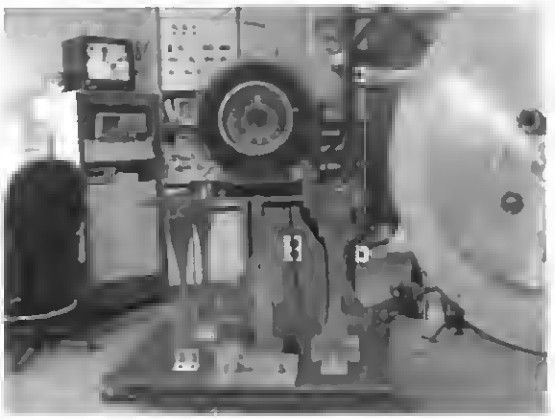

FIGURE 6. MPD Thruster Mounted to Thrust Stand.

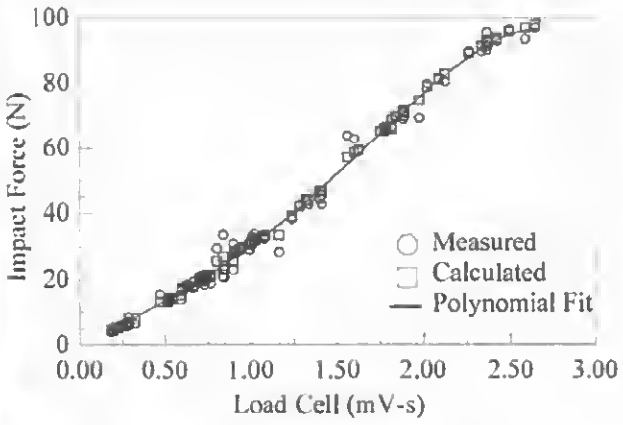

FIGURE 7. Thrust Stand Calibration Curve.

Applied-Field Magnet

Prior research has shown that it may be advantageous to operate MPD thrusters with axial and radial magnetic fields provided by extemal solenoid magnets (Sovey, 1988; Myers, 1991; Mikellides 2000a; 2000h). Although not used in the preliminary performance data reported below, this option is available through the use of an un-cooled magnet consisting of insulated 4-AWG copper cabling wound on a 0.2-m (8") OD pvc pipe. The insulated cahling is continuously wound in 7 layers, with 18 turns per layer. Because the magnet is not cooled, both the maximum current and the period of operation are limited; however, the simplicity of operation and the field strength achieved over the short thruster pulse period outweigh these disadvantages. Power is supplicd by a 50-kW constant-current arc welder, capable of delivering up to 1000 A to the magnet. The measured axial magnetic field strength at the center of the magnet coil is roughly $5x10^{-4}$ T/A, while at the end of the coil the axial field along the centerline is approximately $3.3x10^{-4}$ T/A.

Control System

The events leading up to a pulsed thruster discharge are controlled with an automated sequencing system mounted in the MPD control rack. If the applied-field magnet is to be used, the magnet power supply is preset to the desired current level. The capacitor bank is then charged to the desired voltage using a 4-kW, 10-kV power supply located in the control rack. Once the bank is charged to the desired voltage, the charging supply is disengaged and the test sequence is initiated. For applied-field operation, the magnet power is turned on for a period of 4.5 s, sufficient to establish a constant field distribution within the thruster and to allow any residual thrust stand disturbances due to switching on the magnet to damp away. Toward the end of this period, a timer activates the propellant plenum solenoid to provide gas flow to the thruster; as noted, the duration of the gas pulse can be set from 90-ms to 150-ms, with the present value set at 110-ms to ensure proper gas flow to the thruster. The capacitor bank switch is triggered at the end of the gas pulse timer, providing an approximately 2-ms, high current discharge to the thruster. Once the bank has fired, the control sequence turns off the gas flow, waits approximately 500 milliseconds and turns off the magnet current (to prevent magnet tare forces from interfering with thruster data collection), and then the logic system automatically resets to initiate another test sequence.

Data Collection

The primary diagnostics at this stage of facility development include thruster voltage and current, thrust stand displacement, and magnet coil temperature. Thruster voltage and current are used to calculate the thruster power. Voltage, current, thrust, and mass flow rate are combined to determine thruster efficiency, η:

$$\eta = \frac{T^2}{2\dot{m}VJ} \tag{1}$$

where T is the thrust (N), $\dot{m}$ is the propellant mass flow rate (kg/s), V is the discharge voltage, and J is the thruster operating current.

Digital oscilloscopes measure and record the thruster voltage, thruster current, and load cell voltage waveforms, which are then transferred to a desktop computer for later analysis. Differential voltages are measured across the thruster electrodes using a voltage attenuation (resistor network) circuit to scale the voltage channels and prevent waveform clipping by the oscilloscopes. The differential voltage is measured over a 500-μs period in a quiescent portion of the 2-ms discharge, with a typical uncertainty of ± 5%. Two independent current monitors (transformers) are used to record the pulsed current into and out of the thruster. The coils are rated for 50-kA peak current, a current-time product of 65 A-s, and a rise time of 2.5×10^{-7} s. The discharge current is measured over the same 500-μs period as the differential voltage; due to slight rippling in the current waveform, the measurement uncertainty in the discharge current is approximately ±5%.

The temperature of the thruster is not expected to increase significantly during each 2-ms discharge, and the period between pulses is sufficiently long (~ minutes) so that thruster electrode temperature measurements are not required. However, the coil current will resistively heat the magnet during the few seconds of operation required for applied-field MPD thruster tests, hence thermocouples have been embedded in the coil to monitor the temperature rise and to signal when testing should be suspended to cool the magnet. Although no plasma diagnostics are currently in place, plans call for the installation of Hall and Langmuir probes to provide density and temperature measurements in the thrust chamber and plume region.

Baseline MPD Thruster

Based on numerical simulations using a GRC MPD thruster code (LaPointe, 1992; 1994), a laboratory-model MPD thruster was designed and fabricated and is undergoing initial testing in self-field mode over power ranges from a few hundred kilowatts up to a few megawatts. Shown in Fig. 8, the GRC baseline thruster employs an anode lip, similar in design to the Princeton University benchmark MPD thruster (Choueiri, 1998). The baseline thruster anode is constructed of stainless steel, with disks bolted together to form the anode chamber and the constricted lip region. The chamber depth is approximately 5.2 cm from backplate to anode face, with an internal chamber radius of

5.7 cm. Tbe anode lip differs from the Princeton benchmark design, and is currently set at 3.8 cm long and 2.5 cm deep. A 0.95-cm radius tungsten rod cathode extends approximately 4.8-cm from the backplate, ending in a 45° conical tip. The electrically insulating backplate separating the anode and cathode is composed of boron nitride. A propellant injection ring with a mean radius of 4-cm fits within a circular groove in the boron nitride; propellant enters the thruster through ten evenly spaced holes, each 1/16" (0.15 cm) in diameter, drilled in the downstream face of the ring. The thruster assembly is mounted within the solenoid magnet (Fig. 9), and the wbole assembly is bolted to the top plate of the thrust stand.

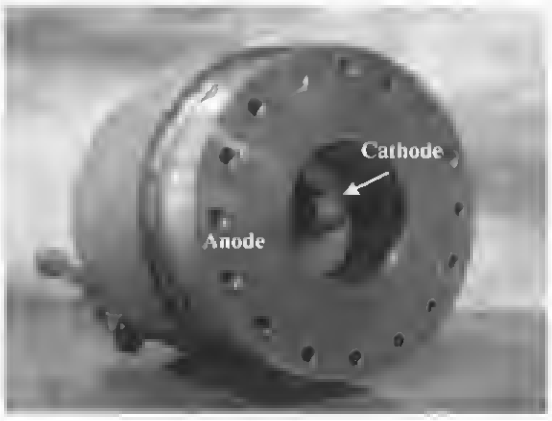

FIGURE 8. Baseline MPD Thruster.

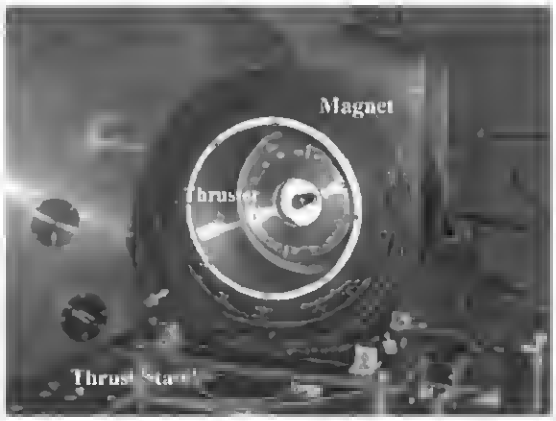

FIGURE 9. MPD Thruster Mounted in Solenoid Magnet.

Quasi-Steady vs. Steady-State

ldcally, high power MPD thruster tests would be performed using continuous power in steady-state operation to address both performance and lifetimc issucs; however, the present lack of available domestic vacuum facilities designed for continuous operation at megawatts of power and gram per second propellant mass flow rates precludes near term steady-state ground testing. As evidenced by prior high power plasma thruster research, a suitable cost-effective option is to operate MW-class thrusters in a quasi-steady or pulsed mode, where each discharge lasts on the order of milliseconds. Although short, the duration of each pulse is sufficient to ionize and accelerate the plasma propellant in a manner similar to that of a true steady-state device (Clark, 1970). However, a key difference between high power operation in pulsed and steady-state modes is that electrode voltages are somewhat higher and the total thrust is lower during pulsed thruster operation (Auweter-Kurtz, 1988; 1993). Such discrepancies can be traced to the cooler electrode temperatures inherent in pulsed devices, which do not provide the same thermionic emission or thermal thrust contributions achieved in steady-state operation. In terms of measured thruster efficiency, these discrcpancies lead to an under-prediction of the total device efficiency (Eqn 1). That it yields an under-prediction is advantageous, since a steady-state device operated at the same discharge conditions would be expected to bave higher total thruster efficiency.

A second key difference between pulsed and steady state operation is that the cathode surface in a pulsed thruster undcrgoes significantly higher erosion than a cathode operated in steady-state mode. This is again attributable to the lower temperature of the cathode surface, which results in cold-cathode spot current emission instead of the more uniform thermionic emission achieved with hot cathodes. As such, reliable measurements of MPD cathode lifetime cannot be made based on pulsed, bigh-power thruster operation. These electrode erosion issues must be addressed to demonstrate adequate thruster lifetime, but the low technology readiness level of current MPD thrusters suggests that a near-term focus on improving thruster efficiency is warranted as a first step for these devices to be considered a viable in-space propulsion option.

PRELIMINARY TEST RESULTS

Commissioning the test facility and reducing the tares on the pulsed high power thrust stand took a significantly longer period of time than anticipated, and only a limited amount of experimental data bas been collected to date. As such, the data presented here is provided only to illustrate the present measurement capabilities of the quasi-steady test facility, with the understanding that additional experimental data will be obtained over the next several months to more fully characterize baseline MPD thruster performance.

Figures 10a and 10b show the response of the thrust stand to cable tare forces generated at discbarge currents of 6-kA and 12-kA, respectively, obtained using a shorting cable across the electrode connections. The higher frequency hash appearing on the measurements is due to ambient facility noise. A negligible tare force is observed at 6-kA, while at 12-kA the integrated load cell response is below 0.1-mVs. The measurement of tare forces over the full range of discbarge currents has yet to be completed, but the values obtained to date are very repeatable and account for less than a few percent of the anticipated mV-s response values (Fig. 7) that will be generated during thruster operation.

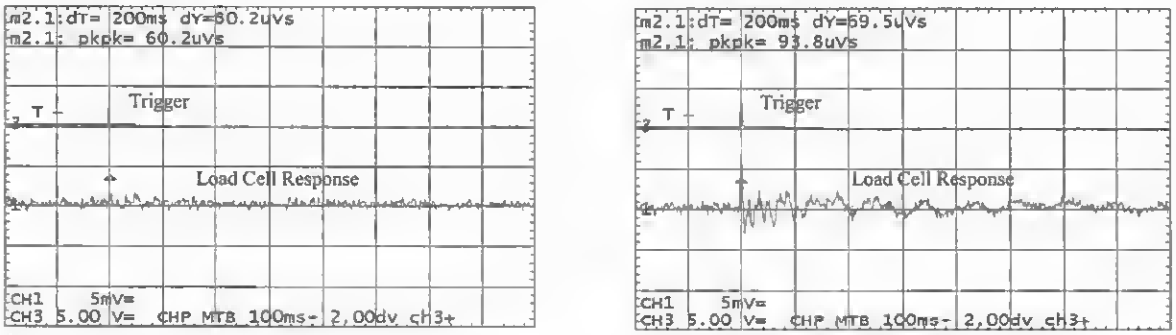

(a) Current = 6-kA. (b) Current = 12-kA.

FIGURE 10. Load Cell Response to Cable Motion During Capacitor Bank Discharge.

Figure 11a shows the response of the thrust stand to a 150-ms pulse of cold argon gas at an equivalent propellant flow rate of 0.5-g/s, and Figure 11b shows the thrust stand response for an equivalent argon propellant mass flow rate of 1.0-g/s (note the change in scale between the two figures). The integrated time response of the load cell to the pulsed propellant flow rates are approximately 0.27-mVs and 0.81-mVs, respectively, and the integrated values are generally repeatable to within a few percent from shot to shot. Again, hash due to vacuum pump operation and ambient facility noise is apparent on each trace. As shown in Figure 7, the integrated load cell response to cold gas flow can be a significant fraction of the anticipated load cell response at low thrust (low discharge current), hence cold gas measurements (with inherent facility noise) are taken after each thruster shot to obtain the most accurate values. Cable tare forces and the cold gas flow response of the thrust stand are subtracted from thruster impulse measurements prior to calculating actual thrust.

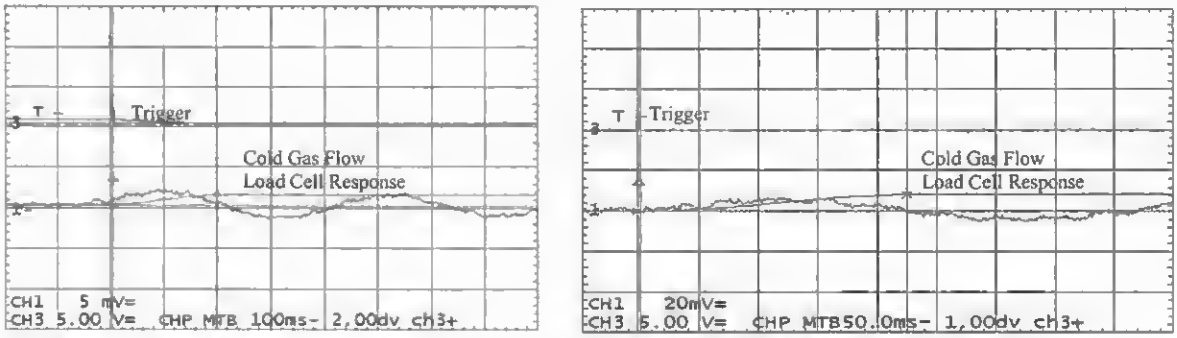

(a) 0.5-g/s. (b) 1.0 g/s (note change in CH1 load cell scale).

FIGURE 11. Load Cell Response to Propellant Gas Flow.

Figure 12a shows the thrust stand response for the quasi-steady baseline MPD thruster operating with 0.5-g/s of argon propellant at a current of approximately 7-kA. The initial oscillations in the load cell response are an artifact of mechanical vibrations induced in the thrust stand by the sudden impulse; similar oscillations are observed during calibration trials using the impact hammer. Efforts are currently underway to reduce these initial oscillations, which, although incorporated into the thrust stand calibrations, diminish the accuracy of the integrated impulse values. The integrated load cell value of 0.37-mVs shown in Fig. 12a includes the cold gas and tare forces; once these values have been subtracted, the remaining time integrated impulse due only to the thruster discharge is approximately 0.12-mVs. Based on the thrust stand calibration curve, this corresponds to an equivalent thrust of around 11.7-N.

Shown in Figure 12b is the PFN trigger signal, thruster current trace, and thruster differential voltage waveform for this test shot. Values for thruster current and voltage are measured during a 500-μs period near the end of the traces (as marked by the vertical cursor lines) to better approximate uniform, quasi-steady operation. The calibrated thruster current is 7040-A, and the terminal voltage is 106-V, yielding a discharge power of approximately 750-kW. The efficiency of the thruster, calculated using Equation 1, is around 18.3%, and the specific impulse at this operating condition is approximately 2390 s.

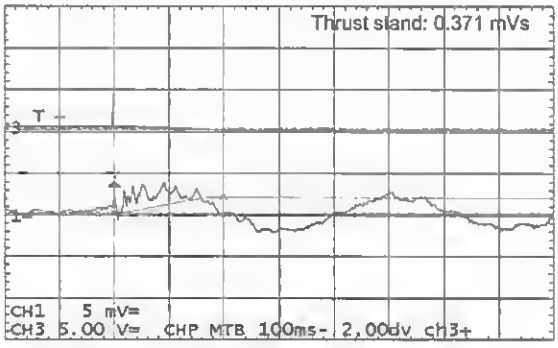

(a) Thrust Stand Load Cell Response.

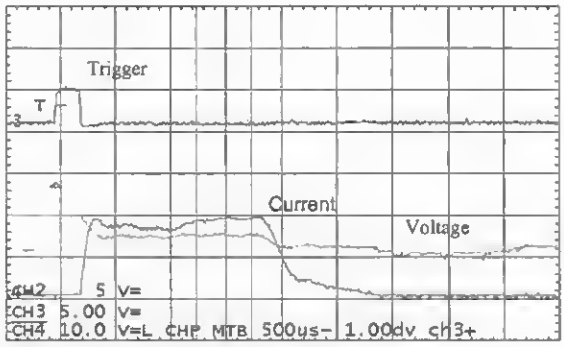

(b). Trigger, Current, and Voltage Traces.

FIGURE 12. 750-kW Test of Baseline MPD Thruster, 0.5-g/s (Ar).

Figure 13a shows the thrust stand response for the baseline thruster operating with 0.5-g/s (argon) at higher power. The calibrated thrust, once the tare forces and cold gas impulse are subtracted, is approximately 21.3-N. The initial oscillations observed on the load cell are more severe than those present at lower power levels, limiting the accuracy of the integrated impulse value. These mechanical vibrations are currently being evaluated, and the thrust stand is being redesigned to substantially reduce these vibrations prior to taking additional high power thruster data. Figure 13b displays the PFN trigger, discharge current, and differential voltage waveforms. As before, the voltage and current values are measured over the last 500-μs of the discharge period. The voltage for this test shot is 167-V, the current is 10-kA, and the corresponding power is 1.67-MW. The specific impulse is thus around 4350-s, and the thruster efficiency has improved to 27%. The current and voltage waveforms still appear fairly smooth, indicating the thrust is operating below the onset of instabilities.

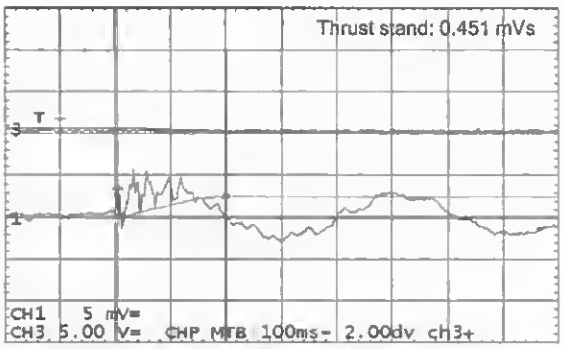

(a) Thrust Stand Load Cell Response.

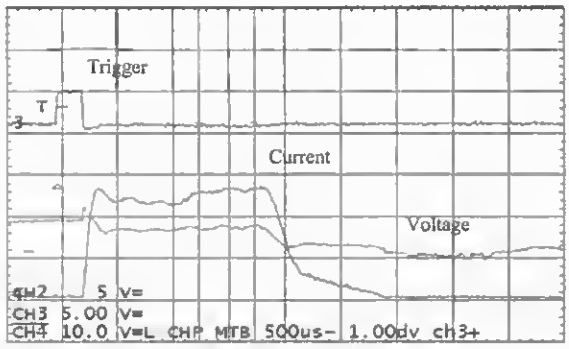

(b) Trigger, Current, and Voltage Traces.

FIGURE 13. 1.68-MW Test Baseline MPD Thruster, 0.5 g/s (Ar).

Although higher discharge powers have been achieved during this preliminary test sequence, the occurrence of initial oscillations in the thrust stand signal limits the accuracy of the load cell data. In addition, the results presented here have not yet been repeated to evaluate the consistency of the baseline thruster performance. These preliminary results are presented primarily to illustrate the present performance of the high power test facility, while a more complete and accurate set of thruster measurements awaits the elimination of the initial load cell oscillations and the repetition of voltage, current, and thrust measurements over a full range of discharge powers.

CONCLUDING REMARKS

A facility to test high power MPD thrusters has been established at NASA GRC, and is currently being used to evaluate the quasi-steady performance of a baseline MPD thruster at pulsed power levels from 500-kW to 5-MW. Preliminary test results have been obtained with argon propellant, and modifications are being made to the impulse-driven thrust stand to reduce initial mechanical vibrations. Near-term plans are to measure a full set of baseline thruster performance data from power levels of 500-kW to the onset of instabilities. This data set will be used to validate MPD thruster modeling results, and to serve as a reference against which to measure performance changes due to modifications in thruster design. The advantage of the pulsed test facility is that it permits the rapid and economical evaluation of high power MPD thruster design variations to meet the goal of improving thruster efficiency, prior to embarking on more expensive steady-state performance testing to improve thruster life. In support of the experimental effort, the MACH2 magnetohydrodynamics code is being modified and used at Arizona State University to gain deeper insight into self-field and applied-field MPD thruster physics. In support of future thruster simulations, Kettering University is developing an electrode sheath voltage model for incorporation into the MACH2 code. The experience gained in operating the baseline MPD thruster, coupled with the improved understanding provided by the MACH2 numerical simulations, is expected to lead to the near-term development and demonstration of highly efficient MW-class MPD thrusters.

ACKNOWLEDGMENTS

Technical contributions by the Ohio Aerospace Institute, Arizona State University, and Kettering University are gratefully acknowledged. The authors also wish to thank Gene Strzempkowski, Joseph Dick, James Coy, Donna Neville, Dennis Rogers, and George Readus for mechanical and electrical support during the performance of this research effort.

REFERENCES

Auweter-Kurtz, M., "Plasma Thruster Development Program at the IRS," *Acta Astronautica*, 32 (5), 377-391, 1994.

Auweter-Kurtz, M., Boie, C., Kaeppeler, H., Kurtz, H., Schrade, H., Sleziona, P., Wager, H., and Wegmann, T., "Magnetoplasmadynamic Thrusters – Design Criteria and Numerical Evaluation," *International Symposium on Simulation and Design of Applied Electromagnetic Systems*, Sapporo, Japan, Jan 26-30, 1993.

Auweter-Kurtz, M., Epple, J., Habiger, H., Kurtz, H., Loesener, O., Messerschmidt, E., and Mulzer, D., "Steady State MPD Devices for Reentry Simulation," IEPC-88-114, *20th International Electric Propulsion Conference*, Garmisch-Partenkirchen, W. Germany, Oct 1988.

Clark, K. E. and Jahn, R. G., *AIAA Journal*, 8, pp. 216-220 (1970).

Choueiri, E. and Zeimer, J., "Quasi-Steady Magnetoplasmadynamic Thruster Measured Performance Database," AIAA-98-3472, *34th AIAA/ASME/SAE/ASEE Joint Propulsion Conference*, Cleveland, OH, July 1998.

Filliben, J. D., "Electric Propulsion for Space Applications," Report CPTR96-64, Chemical Propulsion Information Agency, Columbia, MD, 1996.

Gilland, J., "Mission and System Optimization of Nuclear Electric Propulsion Vehicles for Lunar and Mars Missions," NASA CR-189058, Dec 1991.

Gilland, J. and Oleson, S., "Combined High and Low Thrust Propulsion for Fast Piloted Mars Missions," NASA CR-190788, Nov 1992.

Gilland, J., "MPD Thruster Performance Models for System and Mission Analysis," AIAA-2003-4841, *39th AIAA/SAE/ASME/ASEE Joint Propulsion Conference*, Huntsville, AL, July 2003.

Kagaya, Y., Moriyami, M., Tahara, H., Yoshikawa, T., "Effect of Applied Magnetic Nozzle in a Quasi-Steady MPD Thruster," IEPC-2003-31, *28th International Electric Propulsion Conference*, Toulouse, France, March 2003.

Kinefuchi, K., Toki, K., and Funaki, I., "Nozzle Shape Effects on Velocity Distribution in an MPD Arcjet," IEPC-2003-56, *28th International Electric Propulsion Conference*, Toulouse, France, March 2003.

Kodys, A., Cassady, L., and Choueiri, E., "Performance of a 30-kW Applied-Field Lithium Lorentz Force Accelerator,", AIAA-2003-4842, *39th AIAA/SAE/ASME/ASEE Joint Propulsion Conference*, Huntsville, AL, July 2003.

Kodys, A., Emsellem, G., Cassady, L., Polk, J., and Choueiri, E., "Lithium Mass Flow Control for High Power Lorentz Force Accelerators," *Space Technology and Applications International Forum (STAIF) 2001*, edited by M. El-Genk, AIP Conference Proceedings 552, Melville, NY, 2001, pp. 908-915.

LaPointe, M. R. and Mikellides, G., "Design and Operation of MW-Class MPD Thrusters at the NASA Glenn Research Center," AIAA-2002-4133, *38th AIAA/SAE/ASME/ASEE Joint Propulsion Conference*, Indianapolis, IN, July 2002.

LaPointe, M. R., "Numerical Simulation of Geometric Scale Effects in Cylindrical Self-Field MPD Thrusters," AIAA-92-3297, *28th AIAA/SAE/ASME/ASEE Joint Propulsion Conference*, Nashville, TN, July 1992.

LaPointe, M. R., "Numerical Simulation of Cylindrical, Self-Field MPD Thrusters with Multiple Propellants," NASA CR-194458, January 1994.

Mikellides, P. G., *Theoretical Investigation of Magnetoplasmadynamic Thrusters*, PhD Dissertation, Department of Aeronautical and Astronautical Engineering, Ohio State University, 1994.

Mikellides, P. G., Turchi, P. J., and Roderick, N. F., *J. Propulsion and Power*, 16 (5), 887-893 (2000a).

Mikellides, P. G., and Turchi, P. J., *J. Propulsion and Power*, 16 (5), 894-901 (2000b).

Myers, R., Mantenieks, M., and LaPointe, M., "MPD Thruster Technology," NASA TM-105242, 1991.

Nerheim, N. and Kelly, A., "A Critical Review of the Magnetoplasmadynamic Thruster for Space Applications," NASA CR-92139, Feb 1968.

Oleson, S., "Advanced Electric Propulsion for Space Solar Power Satellites," NASA/TM-1999-209307, Aug 1999.

Paganucci, F., Rossetti, P., Andrenucci, M., Tikhonov, V., and Obukhov, V., "Performance of an Applied Field MPD Thruster with a Pre-Ionization Chamber," IEPC-2003-302, *28th International Electric Propulsion Conference*, Toulouse, France, March 2003.

Polk, J., Tikhonov, V., Semenikhin, S., and Kim, V., "Cathode Temperature Reduction by Addition of Barium in High Power Lithium Plasma Thrusters," in *Space Technology and Applications International Forum (STAIF) 2000*, edited by M. el-Genk, AIP Conference Proceedings 504, Melville, NY, 2000, pp. 1556-1563.

Sankaran, K., Jardin, S. C., and Choueiri, E. Y., "Study of Plasma Flows in Lithium Lorentz Forced Accelerators Using Numerical Simulations," AIAA-2003-4843, *39th AIAA/SAE/ASME/ASEE Joint Propulsion Conference*, Huntsville, AL, July 2003.

Sovey, J. and Mantenieks, M., "Performance and Lifetime Assessment of Magnetoplasmadynamic Arc Thruster Technology," NASA TM-101293, 1988.

Tikhonov, V., Semenikhin, S., Brophy, J., and Polk, J., "Performance of 130-kW MPD Thruster with an External Applied Field and Lithium as Propellant," IEPC-97-120, *25th International Electric Propulsion Conference*, Cleveland, OH 1997.

Toki, K. and Shimizu, Y., "Study of Low-Power MPD Propulsion for Future High-Power Trend," AIAA-2002-4115, *38th AIAA/ASME/SAE/ASEE Joint Propulsion Conference*, Indianapolis IN, July 2002.

Winter, M., Auweter-Kurtz, M., Heiermann, J., and Wegmann, T., "Experimental and Numerical Comparison of High Power Steadys State MPD Thrusters with Radiation- and Water-Cooled Anodes," IEPC-2003-207, *28th International Electric Propulsion Conference*, Toulouse, France, March 2003.

Zuin, M., Antoni, V., Paganucci, F., Cavazzana, R., Serianna, G., Spolaore, M., Vianello, N., Bagatin, M., Rossetti, P., and Andrenucci, M., "Plasma Fluctuations in an MPD Thruster with and without the Application of an External Magnetic Field," IEPC-2003-299, *28th International Electric Propulsion Conference*, Toulouse, France, March 2003.